Docking of New Designed Compounds Derived from 1,6-Dihydro-1,3,5-triazine-2,4-diamine Toward Quadruple Mutant Plasmodium Dihydrofolate Reductase

Imam Siswanto[1,2], Harno Dwi Pranowo[2,*], and Mudasir[2,]**

[1]*Department of Chemistry, Faculty of Science and Technology, Universitas Airlangga, Kampus C Mulyorejo, Surabaya 60115, Indonesia*

[2]*Department of Chemistry, Faculty of Mathematics and Natural Sciences, Universitas Gadjah Mada, Sekip Utara, Yogyakarta 55281, Indonesia*

* ***Corresponding author:***

email: harnodp@ugm.ac.id[*]; mudasir@ugm.ac.id[**]

Received: October 22, 2018
Accepted: January 2, 2019

DOI: 10.22146/ijc.39943

Abstract: *Resistance to the traditional antifolates is now widespread in* Plasmodium falciparum *and* Plasmodium vivax. *To find the interaction model of some compounds derived from 1,6-dihydro-1,3,5-triazine-2,4-diamine, molecular docking technique was carried out using these compounds ligand and pDHFR as the receptor. Complex ligand and the receptor from Protein Data Bank (PDB ID 1J3K) were chosen as an interaction model between a ligand and its receptor. Each compound was optimized using ab initio methods with 6-311G basis set. Partial charges of ligand were added using AM1-BCC methods. Each ligand was docked to the receptor utilizing Dock6 software. Theoretical prediction based on the binding energy between these compounds as the ligand with pDHFR as receptor resulted in 1 compound, namely 6,6-dimethyl-1-[3-(2-chloro-4,5-dibromophenoxy)propoxy]-1,6-dihydro-1,3,5-triazine-2,4-diamine possessing binding affinity better than that of WR99210 which was known to have good antimalarial activity.*

Keywords: *Amber score; pDHFR; molecular docking; triazine*

■ INTRODUCTION

Malaria is known to be the most significant parasitic disease of humans. There are 5 parasite species that cause malaria in humans, and 2 of these species – *Plasmodium falciparum* and *Plasmodium vivax* – have the greatest threat. It has been reported that there were an estimated 212 million new cases in malaria and an estimated 429,000 cases ended with deaths during 2015, and at the start of 2016, nearly half of the world's population was at risk of malaria [1].

Classically, chloroquine (CQ) has been used widely as a standard antimalarial drug for more than 60 years due to many advantages such as excellent availability, low toxicity, effectiveness and facile preparation [2]. Increasing resistant *P. falciparum* emerged researchers to design and prepare some alternatives such as isoquine and related amodiaquine analogs [3]. Isoquine raised a new problem due to its highly sensitive to form O-glucuronide metabolite, which may affect its accumulation in tissues [4]. Besides chloroquine, pyrimethamine was also used to treat malaria disease. However, pyrimethamine resistance was widely spread over the world. The sulfadoxine-pyrimethamine, a pyrimethamine derivative, resistance was also found in some countries in Asia, Africa, South America and also Indonesia [5]. Pyrimethamine resistance is caused by the gene mutation on the certain parasite encoding dihydrofolate reductase in Plasmodium. This mutation changes the expression and alters protein structure that the pyrimethamine is no longer comply to interact with the active site of dihydrofolate reductase, lowering the binding affinity of pyrimethamine to dihydrofolate reductase and finally reducing antimalaria activity.

Various strategies have been implemented to discover new antimalarial drugs [6]. Some researchers try to find a new antimalarial drug base on the molecular docking study [7-12]. Binding free energy between ligand-receptor of the best pose (conformation) resulted from docking procedure are then calculated via

Molecular Mechanics/Generalized Born Surface Area (MM/GBSA) approach [13-14]. The invention can be performed by testing compounds which are derived from previously mutated *P. falciparum* dihydrofolate reductase (pDHFR) resistance, e.g. pyrimethamine [15], quinazoline derivatives [16] and 2,4-diamino-5-(2'-arylpropargyl) pyrimidine derivatives as antifolate [17]. The invention can also be targeted for hybrid compounds [18-19].

On the search of new compounds criteria, it has been concluded that most of DHFR inhibitor are compounds possessing a nucleus made up from fused heterocyclic substituted with amino groups, for instance, methotrexate (**MTX**) [20]. Another criteria for a compound to be potential pDHFR inhibitor are (i) Hydrogen-bond (H-bond) donor head group possessing ability to interact with amino acid residue Asp54, Ile14 and Leu154, (ii) hydrophobic aromatic tail which occupies the hydrophobic pocket of the active site to enhance inhibitory activity, and (iii) linker unit between the H-bond donor head groups and hydrophobic aromatic tail to provide flexibility, in order to avoid unfavorable steric clashes with Asn108 in the active site of the mutant pDHFR enzyme [21]. Similar criteria but for more specific series of compounds, i.e., triazines and triazaspirodienes derivatives are (i) the presence of the common diaminodiazine motif and (ii) spacer groups such as the 1,3-dioxypropyl that connects the two ring systems [22]. A skeleton which met those criteria can be shown in Fig. 1.

Based on those criteria, we previously evaluated a series of theoretical compounds by means of QSAR (Quantitative Structure-Activity Relationship) analysis to find some compounds possessing high anti-malarial activity indicated by the predicted IC50 lower than 100 μM [22]. This work resulted in 6 recommended compounds as listed in Table 1. Compound number 7 is 6,6-dimethyl-1-[3-(2,4,5-trichlorophenoxy)propoxy]-1,6-dihydro-1,3,5-triazine-2,4-diamine (coded name WRA) which was obtained from crystallographic structure (PDB ID 1J3K) and acts a reference in this work. This research is aimed to find physical information about the interaction between 1,6-dihydro-1,3,5-triazine-2,4-diamine derivatives with quadruple mutant pDHFR.

■ EXPERIMENTAL SECTION

Materials

The receptor model was obtained from the Protein Data Bank (PDB) server (http://www.rcsb.org/) with ID 1J3K [23]. This complex consists of four chains (A–D). Quadruple mutant (N51I+C59R+S108N+I164L) pDHFR enzyme was located in chain A as a complex with WRA then chain A was chosen as a complex model. Dihydro-nicotinamide-adenine-dinucleotide phosphate (NADPH) and crystals of water were stripped out from the complex. The hydrogen atom and atomic charge were added to pDHFR using molecular mechanics method with AMBER ff14SB force field [24].

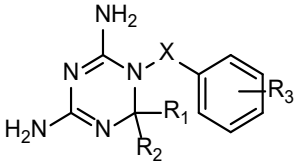

Fig 1. Main skeleton of a series [22]

Table 1. Theoretical compounds with high antimalarial activity and their predicted pIC_{50}

No	Code	R_1	R_2	X	R_3	Predicted	
						IC_{50} (μM)	pIC_{50}
1	Q57	$-(CH_2)_4-$		$-O-(CH_2)_2-O-$	H	2.63×10^{-41}	40.58
2	Q58	$-(CH_2)_4-$		$-O-CH_2-O-$	H	2.09×10^{-11}	10.68
3	Q59	$-(CH_2)_4-$		$-O-(CH_2)_4-$	H	4.57×10^{-12}	11.34
4	W62	CH_3	CH_3	$-O-(CH_2)_3-O-$	2'–Cl–4',5'–diBr	9.55×10^{-58}	57.02
5	W63	CH_3	CH_3	$-O-(CH_2)_3-O-$	2'–Cl–4',5'–diF	9.12×10^{-58}	57.04
6	W64	CH_3	CH_3	$-O-(CH_2)_3-O-$	2'–Br–4',5'–diF	1.66×10^{-57}	56.78

Procedure

Ligand structure preparation

Six ligands resulted in our previous work [25], were built by replacing the groups around the triazine ring (head) marked with R_1 and R_2, linker unit between triazine and the benzene ring (tail) marked with X and groups around the benzene ring marked with R_3. Although R_3 could be Cl, Br, H, OCH_2O, CH_3, OCH_3, C_2H_5, CH_2OH, $CH(CH_3)_2$, C_6H_5 [26], in this work we only used F, Cl, and Br. Ligand models were drawn using HyperChem6 software of HyperCube, Inc (http://www.hyper.com/). All the ligand models were pre-optimized using MM+ molecular mechanics methods before being energetically and geometrically optimized at Hartree–Fock *ab initio* method with 6–311G basis set as implemented in Gaussian09 package program. These optimized ligands were saved in MDL mol file format. Hydrogen atoms and atomic charge were added using the AM1–BCC charge calculation method [24] and loaded using UCSF Chimera program (https://www.cgl.ucsf.edu/chimera/) [27] respectively. All these protonated and charged ligands were saved in Sybil mol2 files format.

Docking parameters validation

Molecular docking was performed using Dock 6.8 software (http://dock.compbio.ucsf.edu/) [28] running on the Linux operating system. Docking studies were carried out on an Intel Xeon 8 Cores E5 2620 v5, with 16 GB memory. The molecular surface of the receptor was generated based on the implementation of the algorithm developed by Richards and Connolly in the included tools of Dock 6.8 distribution. Spheres of the molecular surface were generated using sphgen program that is also included in Dock 6.8 distribution. Since the position of the active site is known from the location of the ligand in a crystal structure, the spheres were selected within 10.0 Angstroms apart from the ligand. The dimension of the grid for ligand sampling were 26.694 Å x 23.718 Å x 28.950 Å with 0.2 Å resolution. The quality of the docking parameters validation was quantified by the root mean square deviation (RMSD) [29].

Ligands docking

All parameters on validation were implemented to carry out ligands docking toward pDHFR as the receptor. Each ligand was docked within the binding site of the receptor using Dock 6.8 resulting in the best pose of the ligand. This best pose was then rescored to obtain binding free energy between ligand and receptor. Hydrogen bonds were analyzed using BIOVIA Discovery Studio Visualizer v17.2.0.16349 with tolerances of 0.4 Å and 20.0 degrees.

Docked ligands rescoring

To refine and calculate binding free energy between ligand and receptor, the best pose of each ligand was then rescored using Amber score. Amber score was configured to perform 100 minimization and 3000 molecular dynamics (MD) simulation steps. The temperature of the simulation system was maintained constant at 300K.

■ RESULTS AND DISCUSSION

Docking Parameters Validation

In order to evaluate the accuracy of the docking procedure, the lowest energy of the ligand predicted by the docking procedure was compared with the experimental binding mode as determined by X-ray crystallography. The docking procedure was validated by removing WRA from the binding site and re-docking it to the binding site of pDHFR. The molecular surface of the receptor was generated with the dms tool which was included in the DOCK 6.8 package program. The molecular surface was obtained by dms tool and spheres of the receptor were generated using sphgen program [30]. The selected spheres as the representation of the binding site and the grid box on the receptor were shown in Fig. 2.

A good agreement between the pose of WRA upon docking and the one from the crystal structure is indicated by the similarity of hydrogen bonding interactions (Fig. 3(a) and (b)), small RMSD 0.707 Å [31] and a slight difference in hydrogen bond length (Table 2). The superimposition between the docked and

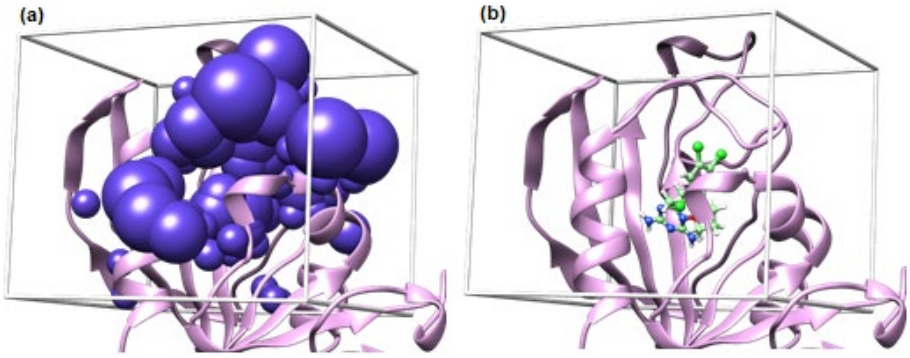

Fig 2. Selected cluster of spheres of the receptor as the representation of the binding site (a) and reference ligand WRA (b) were both inside the grid box. The size of the grid box makes it possible for the ligand to freely move inside the box.

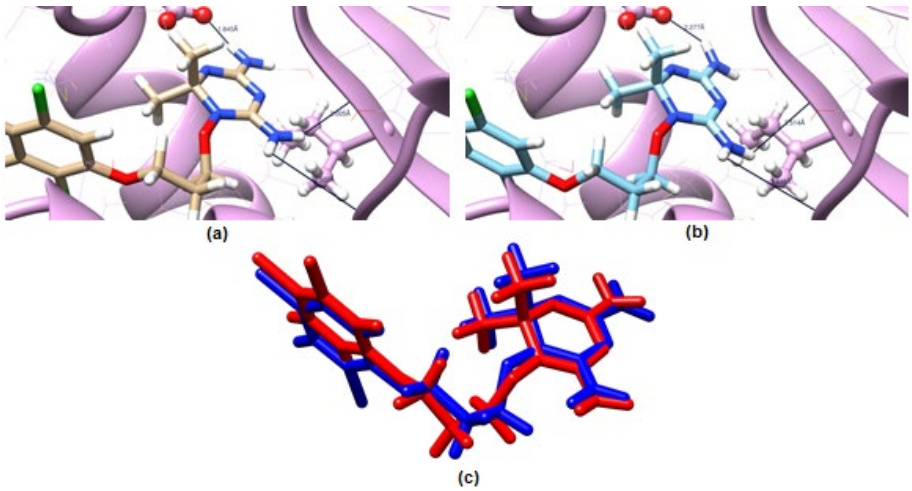

Fig 3. Hydrogen bonds comparison of WR99210 conformation pose originated from the crystal structure, PDB ID 1J3K (a) and that docked by Dock6 (b). Superimposition of the crystallographic (blue) and the docked conformation (red) indicates the similarity position upon docking (c)

Table 2. Hydrogen bonds between WRA and pDHFR from the crystallographic structure and upon docking

Hydrogen bonding	crystal structure (Å)	upon docking (Å)
NH1 – ASP 54	1.845	2.277
NH2 – ILE 14	2.005	2.514
NH2 – LEU 154	2.502	2.448

the observed X-ray crystallographic conformation is shown in Fig. 3(c).

Ligand Docking and Scoring

A series of 9 WRA derivative compounds (including WRA itself) were built and studied to investigate their binding mode within the active or binding site of quadruple mutant pDHFR. Automated docking was carried out without explicit water molecules. Docking was performed on two stages: the first stage was carried out to obtain the best pose of each ligand utilizing grid–based scoring function which is fast and less expensive and while second to refine the docking score resulted from the first stage score [32]. This refinement procedure was carried out by passing each best conformation achieved by grid docking through the second docking stage. This refinement procedure utilized Amber score program which was included in Dock6.8 package program. Amber score was based on Amber molecular dynamics simulation which implemented generalized Born/surface area (GB/SA)

continuum model for solvation free energy [33]. When Amber score program is called, the program performs minimization, MD simulation, and more minimization on the individual ligand, the individual receptor, and the ligand-receptor complex. A single 100 minimization step was performed before the molecular dynamics simulation step. Minimized structures often give as good or better results in MD simulations [34]. It has also been argued that minimization in a GB continuum solvent can save more time [35]. The other advantage of AMBER score is – both the ligand and the active site of the protein can be set to be flexible, allowing small structural rearrangements to reproduce the so-called "induce–fit" while performing the scoring function.

Docking scores of both before and after refinement were listed in Table 3. Correlation between predicted pIC_{50} and refined binding energy was examined using the Spearman correlation test. We found a good correlation between them (ρ = -0.771 and p = 0.072). It was found that 3 compounds (Q57, Q58, and Q59), called group A, had lower binding affinity to pDHFR than the binding activity of WRA while 3 compounds (W62, W63, W64), called as group B, possessed binding energy which was close to the binding energy of WRA. The most stable conformation of all compounds after docking was shown in Fig. 4, while the conformations of 3 ligands inside the active site pocket of the pDHFR possessing lowest binding energy and their detailed

Table 3. Binding energy and interaction formed between ligand and receptor

No	Ligand	H–Bond	Alkyl interaction	Binding energy (kcal/mol)	
				Grid	Amber
1	Q57	SER111	ILE112, PRO113	–13.11	–16.32
2	Q58	–	ILE112, PRO113	–12.80	–13.93
3	Q59	LYS49	ILE112	–12.97	–13.50
4	W62	ILE14, ASP54, LEU164, TYR170	PHE116, PRO113, LEU119, ILE112, LEU46, PHE58	–27.16	–41.73
5	W63	ILE14, ASP54, LEU164, TYR170	PHE58, LEU46, ILE112, PRO113, LEU119	–27.93	–37.06
6	W64	ILE14, CYS15, ASP54, LEU164, TYR170, THR185	LEU46, MET55, PHE58, ILE112, LEU119, PRO113	–29.46	–38.01
7	WRA	ILE14, CYS15, ASP54, LEU164, TYR170, THR185	VAL45, LEU46, MET55, PHE58, ILE112, PRO113, PHE116	–26.11	–39.62

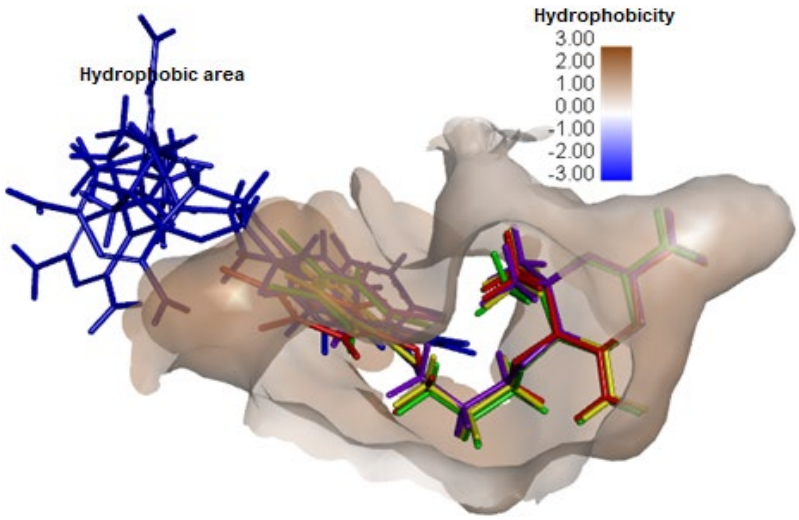

Fig 4. Conformation of ligands upon docking with a lower binding affinity (blue) and higher one: W62 (green), W63 (yellow) and W64 (purple) relative to WRA (red) inside active site pocket of the receptor pDHFR

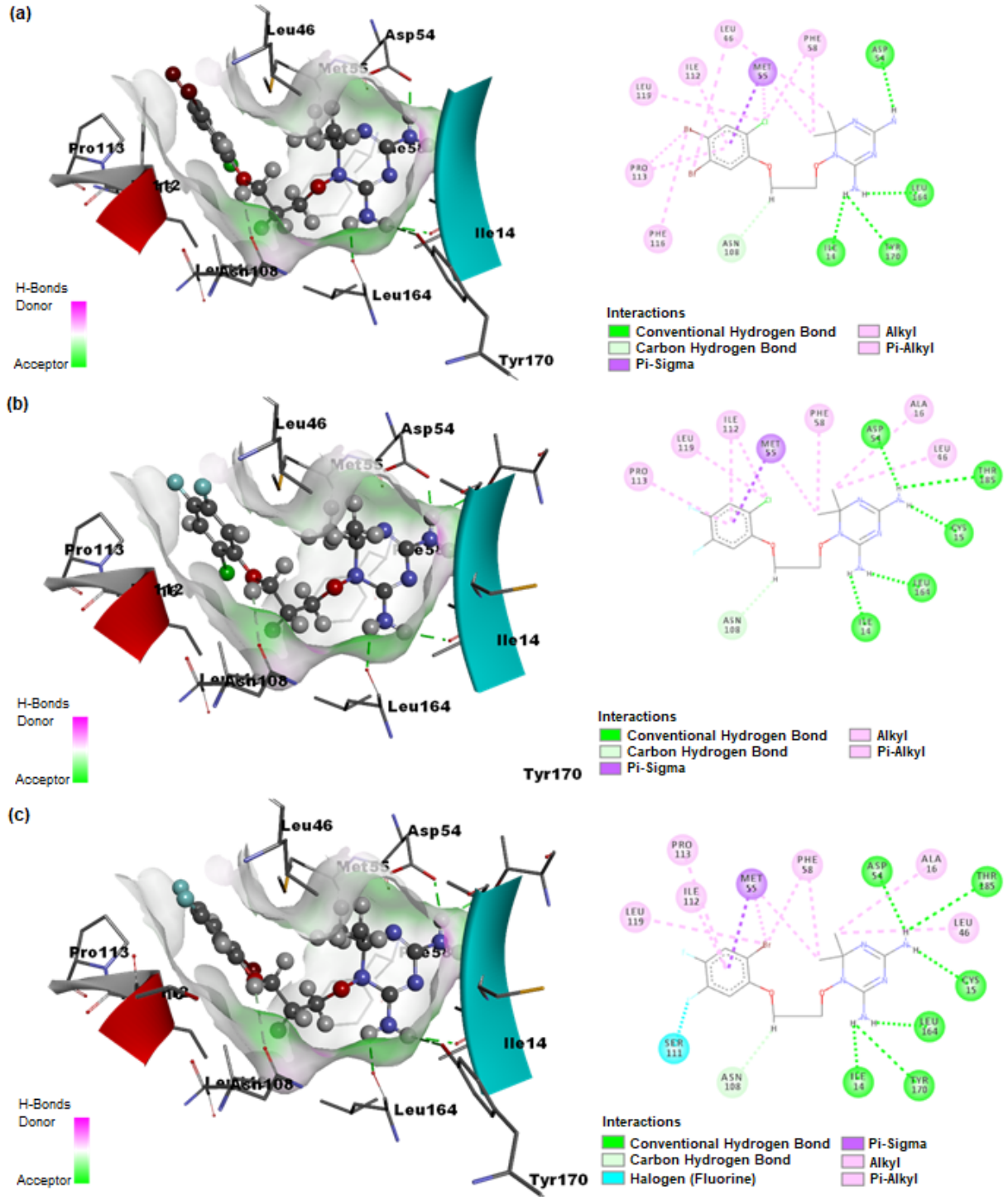

Fig 5. Best pose of ligands upon refinement: (a) W62, (b) W63, and (c) W64 docked toward pDHFR and their related interaction to residues of pDHFR

interaction was shown in Fig. 5(a)–5(c). The detailed interaction of each ligand with pDHFR was reported in Table 3.

Compounds from groups A and B have the same tail of benzene hydrophobic ring with slightly different branches. The hydrophobic portion of groups A and B managed to occupy the same active side hydrophobic pockets (residues Phe58, Met55, Phe116, Pro113, Ile112,

and Ser111). With these residues, group B compound succeeded to form more alkyl interactions than group A. These interactions nevertheless contribute to the binding energy between ligand and receptor.

In contrast, despite having the same hydrophilic ring, group B compounds succeed in approaching the hydrophilic portion of the active side which is largely contributed by ASP54 residue, while group A places its hydrophilic triazine ring in the opposite direction. This position of the triazine ring of group B compound ligand close to hydrophilic pocket makes it possible to form a strong hydrogen bonding between this ligand and the receptor (residues ILE14, ASP54, and LEU164). The linker unit of group B compounds (–O–$(CH_2)_3$–O–) takes place on the stabilization of the binding between ligand and receptor. This stabilization occurs through the formation of van der Waals interaction between the linker units and the ASN108 residue found in the quadruple mutant pDHFR. The presence of this ASN108 residue in the quadruple mutant pDHFR for group A compounds can cause clashing with the linker unit, as a consequence, void the hydrophilic (head) ligand portion to approach the pDHFR hydrophilic pocket receptor [21].

Hydrogen bond analysis reveals that group B compound possesses hydrogen bond modes which are almost similar to hydrogen bonds which are formed between WRA and pDHFR while hydrogen bond of group A is very weak. This weak hydrogen bond is due to the disability of group A to fit the active site pocket of pDHFR. Consequently, group A compounds possess lower binding activity indicated by their binding energy which is less negative compared to that of group B compounds. The strongest binding energy was owned by compound W62 which was more negative even if compared to WRA as a reference compound. This binding energy suggests that compounds of W62 are predicted to be a potential compound for antimalarial drugs candidate.

■ CONCLUSION

A series of compounds derived from 1,6–dihydro–1,3,5–triazine–2,4–diamine has been studied by using molecular docking simulations in order to search alternative compounds for future antimalarial drugs candidates. Among six compounds which have been investigated, three compounds, namely: (a) 6,6-dimethyl -1-[3-(2-chloro-4,5-dibromo-phenoxy)propoxy]-1,6-dihydro-1,3,5-triazine-2,4-diamine, (b) 6,6-dimethyl-1-[3-(2-chloro-4,5-difluorophenoxy)propoxy]-1,6-dihydro -1,3, 5-triazine-2,4-diamine, (c) 6,6-dimethyl-1-[3-(2-bromo-4,5-difluorophenoxy)propoxy]-1,6-dihydro-1,3,5 -triazine-2,4-diamine possess almost similar hydrogen bonding to those formed between WRA (reference compound) and quadruple mutant pDHFR. Furthermore, one compound, i.e. 6,6-dimethyl-1-[3-(2-chloro-4,5-dibromophenoxy)propoxy]-1,6-dihydro-1,3,5-triazine-2,4-diamine shows best binding affinity to pDHFR indicated by the value of the binding energy which is even lower than that of the reference compound, WRA.

■ ACKNOWLEDGMENTS

The authors would like to offer special thanks to Dr.rer.nat. Ria Armunanto, who, although no longer with us, continues to inspire by his dedication to the students he served. Imam Siswanto would like to acknowledge the Ministry of Research, Technology and Higher Education Republic of Indonesia for supporting this work through "*Penelitian Disertasi Doktor*" funding scheme based on contract number 304/SP2H/LT/DPRM/III/2016.

■ REFERENCES

[1] World Health Organization, 2017, *World Malaria Report 2017*, https://apps.who.int/iris/bitstream/10665/259492/1/9789241565523-eng.pdf.

[2] Fidock, D.A., Rosenthal, P.J., Croft, S.L., Brun, R., and Nwaka, S., 2004, Antimalarial drug discovery: Efficacy models for compound screening, *Nat. Rev. Drug Discovery*, 3 (6), 509–520.

[3] O'Neill, P.M., Mukhtar, A., Stocks, P.A., Randle, L.E., Hindley, S., Ward, S.A., Storr, R.C., Bickley, J.F., O'Neil, I.A., Maggs, J.L., Hughes, R.H., Winstanley, P.A., Bray, P.G., and Park, B.K., 2003, Isoquine and related amodiaquine analogues: A new generation of improved 4–aminoquinoline antimalarials, *J. Med. Chem.*, 46 (23), 4933–4945.

[4] Valverde, E.A., Romero, A.H., Acosta, M.E., Gamboa, N., Henriques, G., Rodrigues, J.R., Ciangherotti, C., and López, S.E., 2018, Synthesis, β–hematin inhibition studies and antimalarial evaluation of new dehydroxy isoquine derivatives against *Plasmodium berghei*: A promising antimalarial agent, *Eur. J. Med. Chem.*, 148, 498–506.

[5] Gatton, M.L., Martin, L.B., and Cheng, Q., 2004, Evolution of resistance to sulfadoxine–pyrimethamine in *Plasmodium falciparum*, *Antimicrob. Agents Chemother.*, 48 (6), 2116–2123.

[6] Mishra, M., Mishra, V.K., Kashaw, V., Iyer, A.K., and Kashaw, S.K., 2017, Comprehensive review on various strategies for antimalarial drug discovery, *Eur. J. Med. Chem.*, 125, 1300–1320.

[7] Sainy, J., and Sharma, R., 2017, Synthesis, antimalarial evaluation and molecular docking studies of some thiolactone derivatives, *J. Mol. Struct.*, 1134, 350–359.

[8] Maurya, S.S., Khan, S.I., Bahuguna, A., Kumar, D., and Rawat, D.S., 2017, Antimalarial activity, heme binding and docking studies of N –substituted 4–aminoquinoline–pyrimidine molecular hybrids, *Eur. J. Med. Chem.*, 129, 175–185.

[9] Bhat, H.R., Singh, U.P., Thakur, A., Ghosh, S.K., Gogoi, K., Prakash, A., and Singh, R.K., 2015, Synthesis, antimalarial activity and molecular docking of hybrid 4-aminoquinoline-1,3,5-triazine derivatives, *Exp. Parasitol.*, 157, 59–67.

[10] Brandão, G.C., Missias, F.C.R., Arantes, L.M., Soares, L.F., Roy, K.K., Doerksen, R.J., de Oliveira, A.B., and Pereira, G.R., 2018, Antimalarial naphthoquinones. Synthesis via click chemistry, in vitro activity, docking to PfDHODH and SAR of lapachol–based compounds, *Eur. J. Med. Chem.*, 145, 191–205.

[11] Debbabi, K.F., Bashandy, M.S., Al-Harbi, S.A., Aljuhani, E.H., and Al-Saidi, H.M., 2017, Synthesis and molecular docking against dihydrofolate reductase of novel pyridin–N–ethyl–N–methyl benzenesulfonamides as efficient anticancer and antimicrobial agents, *J. Mol. Struct.*, 1131, 124–135.

[12] Ugwu, D.I., Okoro, U.C., Ukoha, P.O., Okafor, S., Ibezim, A., and Kumar, N.M., 2017, Synthesis, characterization, molecular docking and *in vitro* antimalarial properties of new carboxamides bearing sulphonamide, *Eur. J. Med. Chem.*, 135, 349–369.

[13] Gálvez, J., Polo, S., Insuasty, B., Gutiérrez, M., Cáceres, D., Alzate-Morales, J.H., De–la–Torre, P., and Quiroga, J., 2018, Design, facile synthesis, and evaluation of novel spiro- and pyrazolo[1,5-c] quinazolines as cholinesterase inhibitors: Molecular docking and MM/GBSA studies, *Comput. Biol. Chem.*, 74, 218–229.

[14] Karaman, B., and Sippl, W., 2015, Docking and binding free energy calculations of sirtuin inhibitors, *Eur. J. Med. Chem.*, 93, 584–598.

[15] Fogel, G.B., Cheung, M., Pittman, E., and Hecht, D., 2008, *In silico* screening against wild–type and mutant *Plasmodium falciparum* dihydrofolate reductase, *J. Mol. Graphics Modell.*, 26 (7), 1145–1152.

[16] Al–Omary, F.A.M., Abou-zeid, L.A., Nagi, M.N., Habib, E.S.E., Abdel-Aziz, A.A.M., El-Azab, A.S., Abdel-Hamide, S.G., Al-Omar, M.A., Al-Obaid, A.M., and El-Subbagh, H.I., 2010, Non–classical antifolates. Part 2: Synthesis, biological evaluation, and molecular modeling study of some new 2,6–substituted-quinazolin-4-ones, *Bioorg. Med. Chem.*, 18 (8), 2849–2863.

[17] Algul, O., Paulsen, J.L., and Anderson, A.C., 2011, 2,4-Diamino-5-(2′-arylpropargyl)pyrimidine deriva tives as new nonclassical antifolates for human dihydrofolate reductase inhibition, *J. Mol. Graphics Modell.*, 29 (5), 608–613.

[18] Chopra, R., Chibale, K., and Singh, K., 2018, Pyrimidine-chloroquinoline hybrids: Synthesis and antiplasmodial activity, *Eur. J. Med. Chem.*, 148, 39–53.

[19] Maurya, S.S., Bahuguna, A., Khan, S.I., Kumar, D., Kholiya, R., and Rawat, D.S., 2019, N-Substituted aminoquinoline-pyrimidine hybrids: Synthesis, *in vitro* antimalarial activity evaluation and docking studies, *Eur. J. Med. Chem.*, 162, 277–289.

[20] Ma, X., and Chui, W.K., 2010, Antifolate and antiproliferative activity of 6,8,10-triazaspiro[4.5]

deca-6,8–dienes and 1,3,5-triazaspiro[5.5]undeca-1,3-dienes, *Bioorg. Med. Chem.*, 18 (2), 737–743.

[21] Adane, L., Bhagat, S., Arfeen, M., Bhatia, S., Sirawaraporn, R., Sirawaraporn, W., Chakraborti, A.K., and Bharatam, P.V, 2014, Design and synthesis of guanylthiourea derivatives as potential inhibitors of *Plasmodium falciparum* dihydrofolate reductase enzyme, *Bioorg. Med. Chem. Lett.*, 24 (2), 613–617.

[22] Ma, X., Xiang, G., Yap, C.W., and Chui, W.K., 2012, 3D–QSAR Study on dihydro-1,3,5–triazines and their spiro derivatives as DHFR inhibitors by comparative molecular field analysis (CoMFA), *Bioorg. Med. Chem. Lett.*, 22 (9), 3194–3197.

[23] Yuvaniyama, J., Chitnumsub, P., Kamchonwongpai san, S., Vanichtanankul, J., Sirawaraporn, W., Taylor, P., Walkinshaw, M.D., and Yuthavong, Y., 2003, Insights into antifolate resistance from malarial DHFR–TS structures, *Nat. Struct. Biol.*, 10 (5), 357–365.

[24] Wang, J., Wang, W., Kollman, P.A., and Case, D.A., 2006, Automatic atom type and bond type perception in molecular mechanical calculations, *J. Mol. Graphics Modell.*, 25 (2), 247–260.

[25] Siswanto, I., Armunanto, R., Pranowo, H.D., and Mudasir, M., 2019, Contribution of the atomic charge of the triazine ring members to the DHFR inhibitory activity using 2D-QSAR, *BMC Proc.*, in press.

[26] Fogel, G.B., Cheung, M., Pittman, E., and Hecht, D., 2008, Modeling the inhibition of quadruple mutant *Plasmodium falciparum* dihydrofolate reductase by pyrimethamine derivatives, *J. Comput.-Aided Mol. Des.*, 22 (1), 29–38.

[27] Pettersen, E.F., Goddard, T.D., Huang, C.C., Couch, G.S., Greenblatt, D.M., Meng, E.C., and Ferrin, T.E., 2004, UCSF Chimera–A visualization system for exploratory research and analysis, *J. Comput. Chem.*, 25 (13), 1605–1612.

[28] Allen, W.J., Balius, T.E., Mukherjee, S., Brozell, S.R., Moustakas, D.T., Lang, P.T., Case, D.A., Kuntz, I.D., and Rizzo, R.C., 2015, DOCK 6: Impact of new features and current docking performance, *J. Comput. Chem.*, 36 (15), 1132–1156.

[29] Allen, W.J., and Rizzo, R.C., 2014, Implementation of the Hungarian algorithm to account for ligand symmetry and similarity in structure-based design, *J. Chem. Inf. Model.*, 54 (2), 518–529.

[30] Kuntz, I.D., Blaney, J.M., Oatley, S.J., Langridge, R., and Ferrin, T.E., 1982, A geometric approach to macromolecule-ligand interactions, *J. Mol. Biol.*, 161 (2), 269–288.

[31] Wang, R., Lu, Y., and Wang, S., 2003, Comparative evaluation of 11 scoring functions for molecular docking, *J. Med. Chem.*, 46 (12), 2287–2303.

[32] Chen, Y.C., 2015, Beware of docking!, *Trends Pharmacol. Sci.*, 36 (2), 78–95.

[33] Genheden, S., and Ryde, U., 2015, The MM/PBSA and MM/GBSA methods to estimate ligand-binding affinities, *Expert Opin. Drug Discovery*, 10 (5), 449–461.

[34] Sun, H., Li, Y., Shen, M., Tian, S., Xu, L., Pan, P., Guan, Y., and Hou, T., 2014, Assessing the performance of MM/PBSA and MM/GBSA methods. 5. Improved docking performance using high solute dielectric constant MM/GBSA and MM/PBSA rescoring, *Phys. Chem. Chem. Phys.*, 16 (40), 22035–22045.

[35] Rastelli, G., Del Rio, A., Degliesposti, G., and Sqobba, M., 2010, Fast and accurate predictions of binding free energies using MM–PBSA and MM–GBSA, *J. Comput. Chem.*, 31 (4), 797–810.